

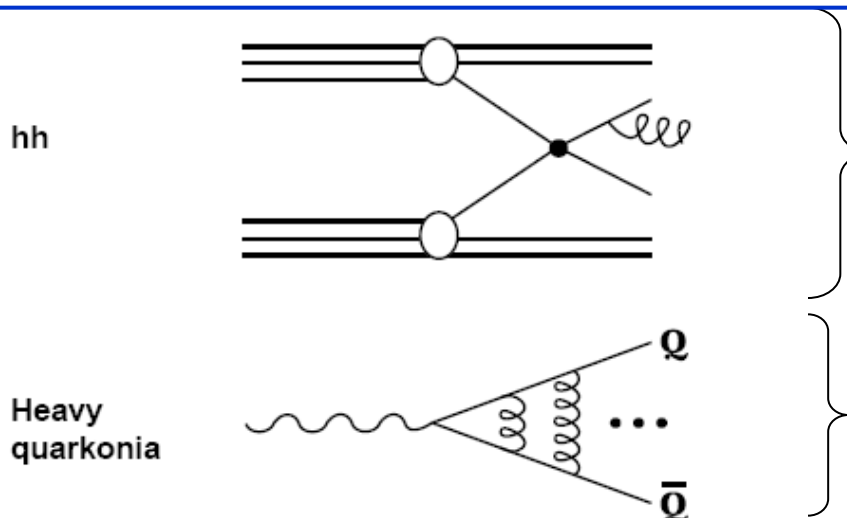
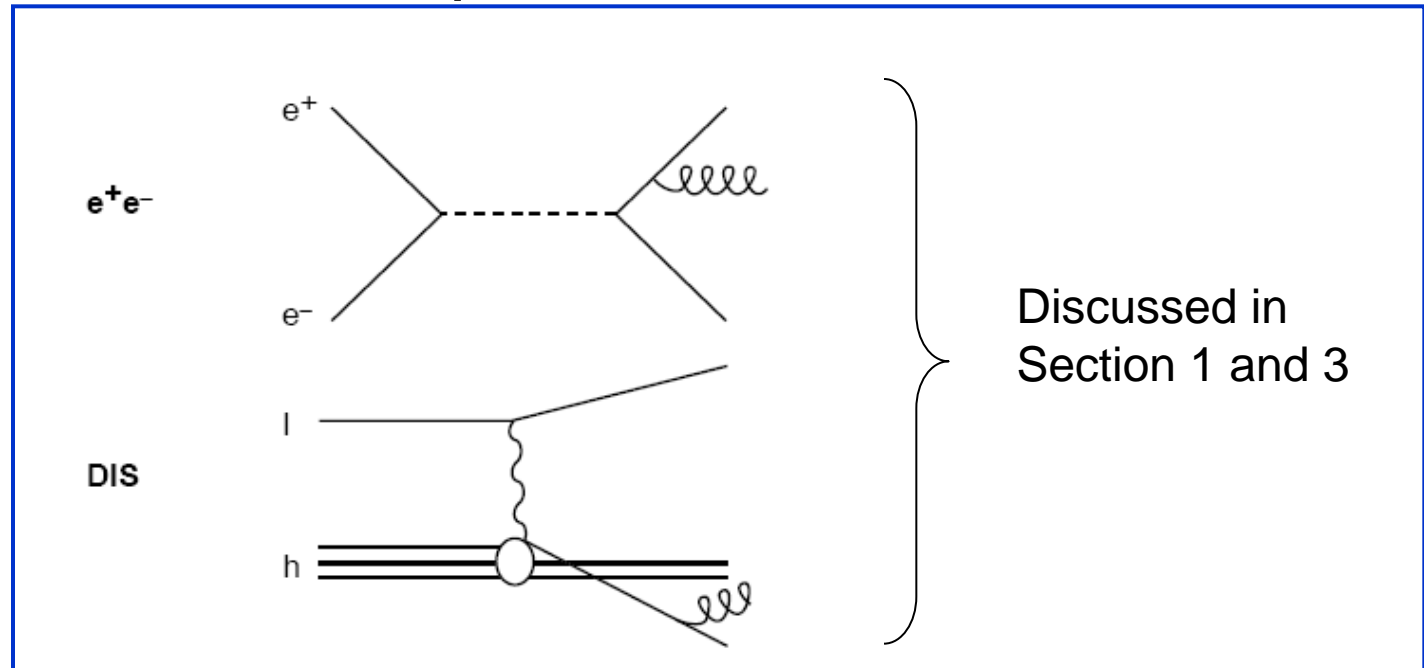
Experimental Tests of QCD

1. Test of QCD in e^+e^- annihilation
2. Running of the strong coupling constant
3. Study of QCD in deep inelastic scattering

Disclaimer:

Due to the lack of time I have selected only a few items!

Test of QCD in different processes

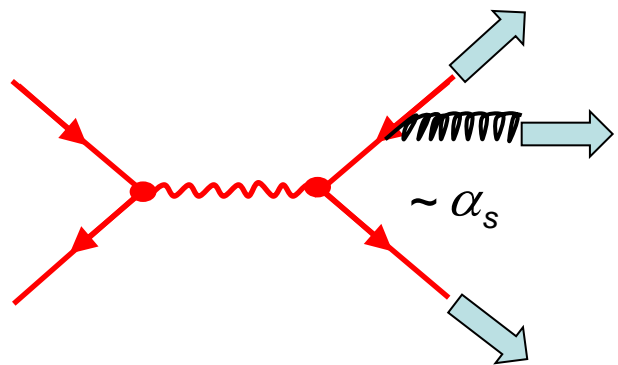


not discussed

1. Test of QCD in e^+e^- annihilation

1.1 Discovery of the gluon

Discovery of 3-jet events by the TASSO collaboration (PETRA) in 1977:



3-jet events are interpreted as quark pairs with an additional hard gluon.

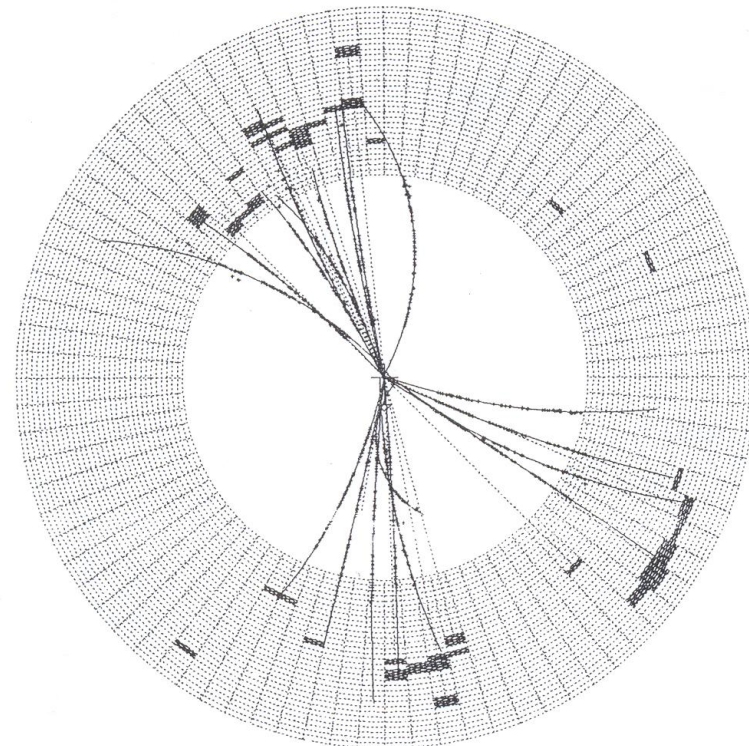


Fig. 11.12 A three-jet event observed by the JADE detector at PETRA.

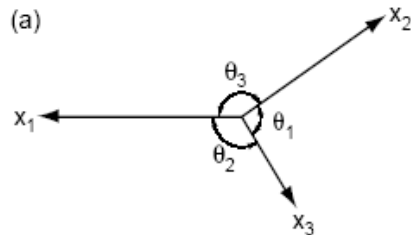
$$\frac{\# \text{3-jet events}}{\# \text{2-jet events}} \approx 0.15 \sim \alpha_s \quad \rightarrow \quad \alpha_s \text{ is large}$$

at $\sqrt{s}=20 \text{ GeV}$

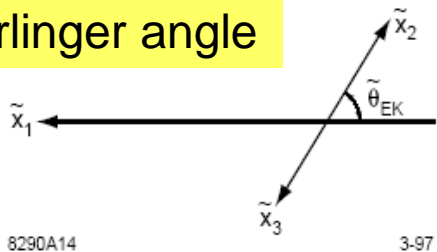
1.2 Spin of the gluon

Angular distribution of jets depend on gluon spin:

Ordering of 3 jets: $E_1 > E_2 > E_3$



Ellis-Karlinger angle



8290A14

3-97

Figure 8: (a) Representation of the momentum vectors in a three-jet event, an (b) definition of the Ellis-Karliner angle.

Measure direction of jet-1 in the rest frame of jet-2 and jet-3: θ_{EK}

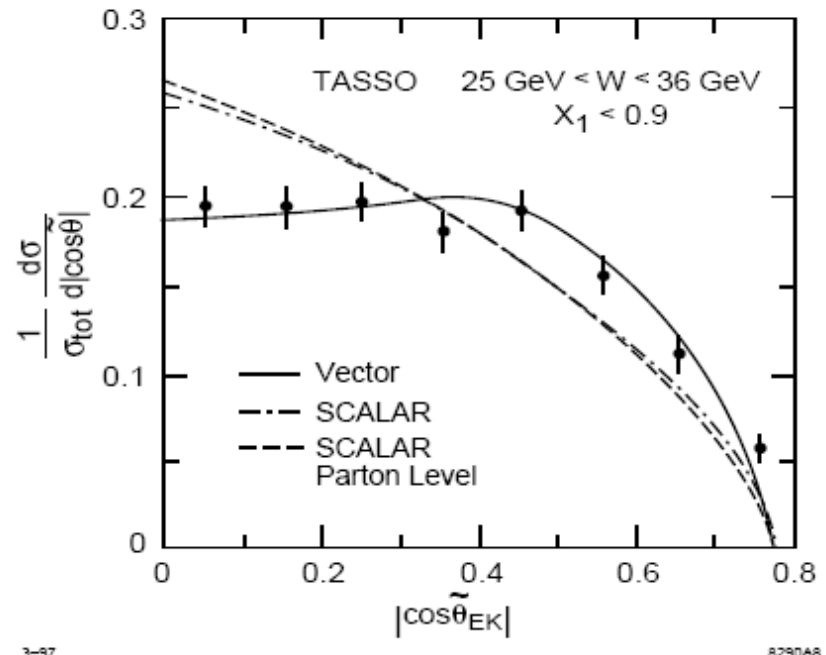


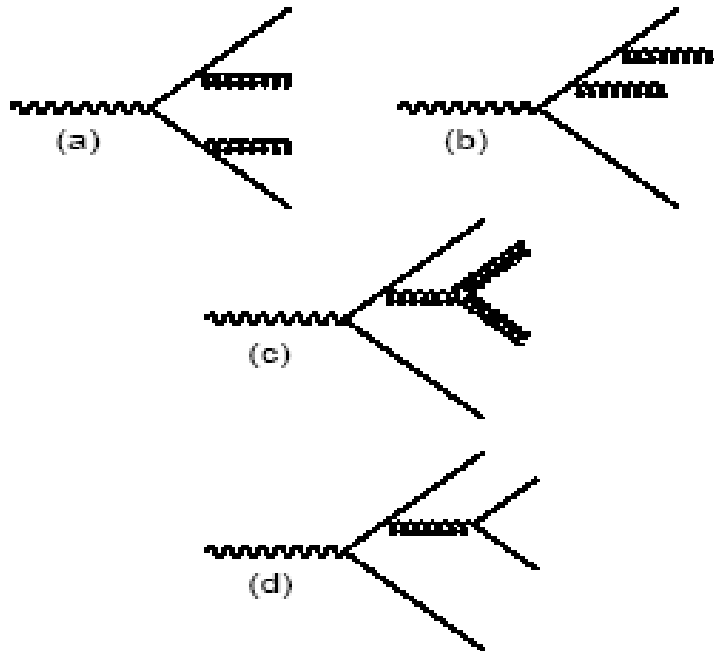
Figure 9: The Ellis-Karliner angle distribution of three-jet events recorded by TASSO at $Q \sim 30 \text{ GeV}$ [18]; the data favour spin-1 (vector) gluons.

Gluon spin $J=1$

1.3 Multi-jet events and gluon self coupling

Non-abelian gauge theory (SU(3))

4-jet events



03-97
5290A.19

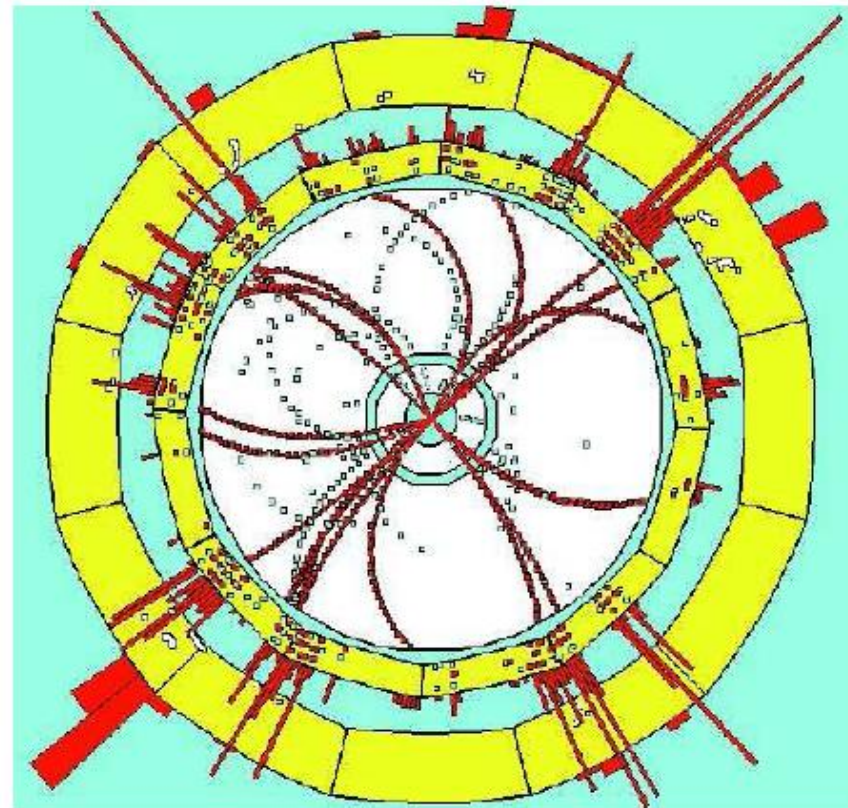


Figure 1: Hadronic event of the type $e^+e^- \rightarrow 4$ jets recorded with the ALEPH detector at LEP-I.

Multi-jet event ALEPH exp (LEP)

→ 4 jet events allow to test the existence of gluon self coupling.

Multiple jets and jet algorithm

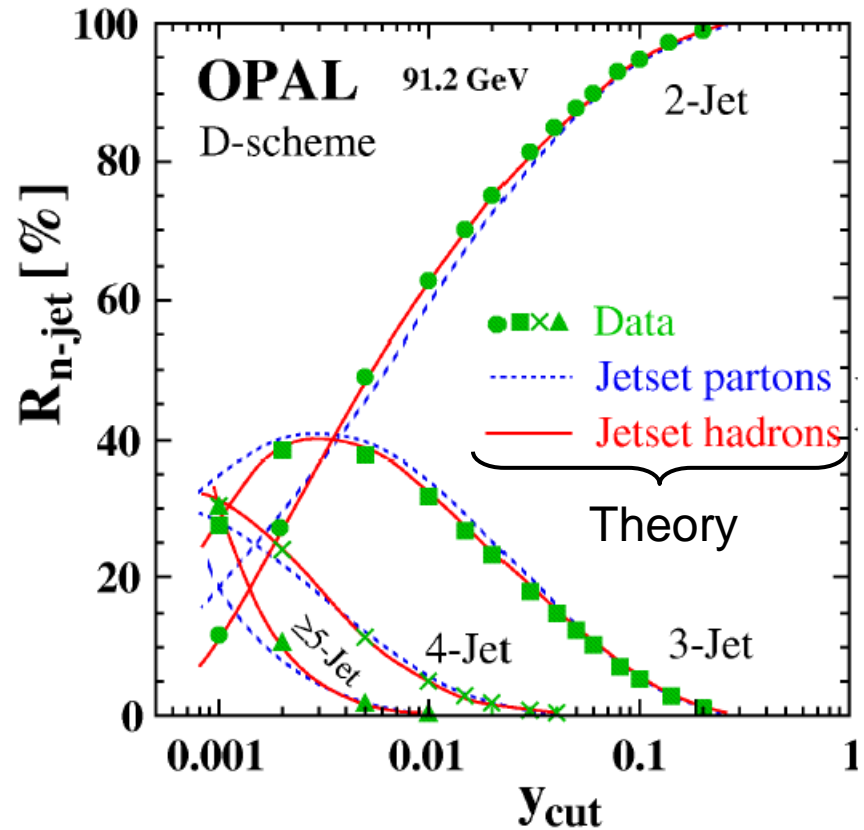
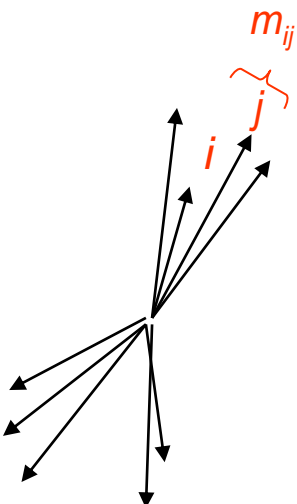
Jet Algorithm

Hadronic particles i and j are grouped to a pseudo particle k as long as the invariant mass is smaller than the **jet resolution parameter**:

$$\frac{m_{ij}^2}{s} < y_{cut}$$

m_{ij} is the invariant mass of i and j.

Remaining pseudo particles are **jets**.



Remark: today, different jet algorithms are used.

Gauge group structure of the strong interaction

Dynamics of gauge theory defined by commutation relation of gauge group generators:

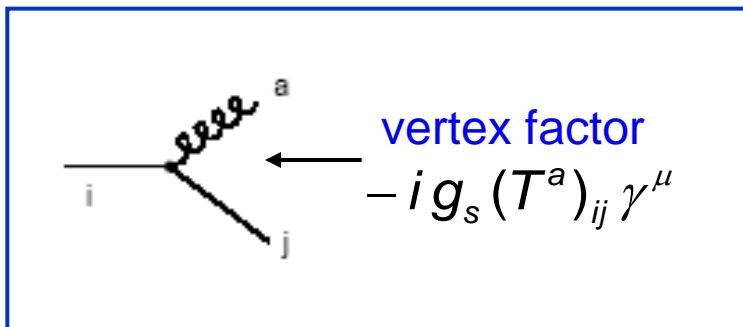
$$[T^a, T^b] = i \sum_c f^{abc} \cdot T^c$$

\uparrow
Structure constants

$$T^a = \frac{\lambda^a}{2}$$

λ^a Gell-Mann matrices

The generators and the structure constants appear in the vertex functions of the Feynman graphs:

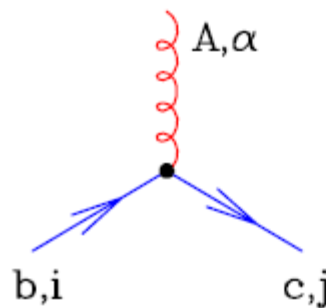


In perturbative calculations the average and sum over all possible color configurations lead to **combinatoric factors**:

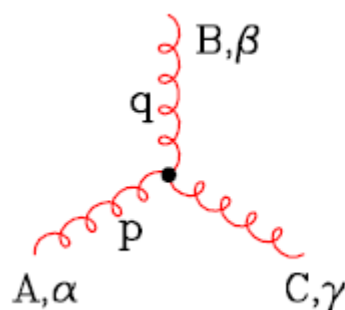
A Feynman diagram showing a vertex where a horizontal line labeled 'i' meets a diagonal line labeled 'j'. A wavy line labeled 'a' enters from the top. A blue arrow points to the vertex with the label "vertex factor". Below the vertex is the expression $(T^a)_{\alpha\eta}(T^a)_{\eta\beta}$.

$$\left| \begin{array}{c} | \\ - \\ \backslash \end{array} \right|^2 \sim \sum_{a=1}^8 \sum_{k=1}^3 (T^a)_{\alpha\eta} (T^a)_{\eta\beta}$$
$$\sum_{k,\eta} T_{\alpha\eta}^k T_{\eta\beta}^k = \delta_{\alpha\beta} C_F = \delta_{\alpha\beta} \frac{4}{3}$$

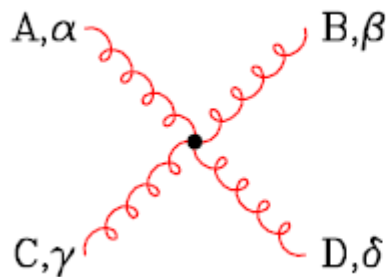
Feynman rules for QCD: vertex factors



$$-ig \ (t^A)_{cb} \ (\gamma^\alpha)_{ji}$$



$$-g \ f^{ABC} [(p-q)^\gamma g^{\alpha\beta} + (q-r)^\alpha g^{\beta\gamma} + (r-p)^\beta g^{\gamma\alpha}]$$

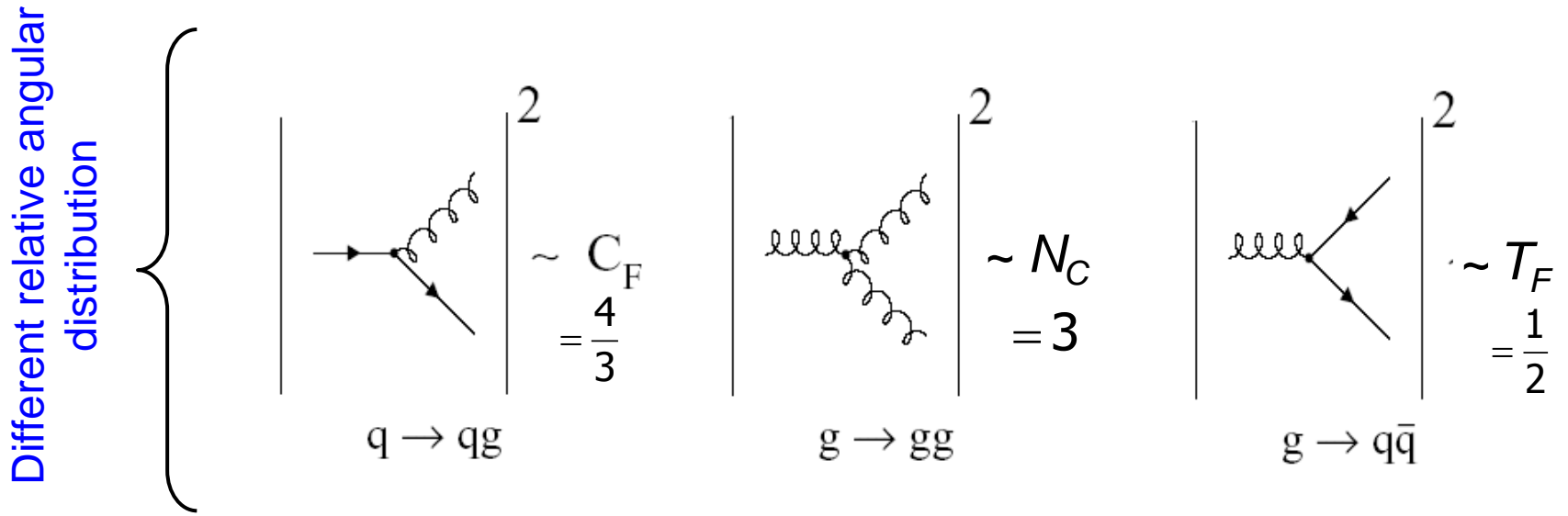


$$-ig^2 f^{XAC} f^{XBD} [g^{\alpha\beta} g^{\gamma\delta} - g^{\alpha\delta} g^{\beta\gamma}]$$

$$-ig^2 f^{XAD} f^{XBC} [g^{\alpha\beta} g^{\gamma\delta} - g^{\alpha\gamma} g^{\beta\delta}]$$

$$-ig^2 f^{XAB} f^{XCD} [g^{\alpha\gamma} g^{\beta\delta} - g^{\alpha\delta} g^{\beta\gamma}]$$

Color factors relevant for 4-jet events



$$\sum_{k,\eta} T_{\alpha\eta}^k T_{\eta\beta}^k = \delta_{\alpha\beta} C_F = \frac{N_C^2 - 1}{2N_C} \cdot \mathbf{1} = \frac{4}{3} \cdot \mathbf{1}$$

$$\sum_{a,b} f^{abc} f^{abd} = \delta_{cd} C_A \quad C_A = N_C$$

$$\sum_{\alpha,\beta} T_{\alpha\beta}^a T_{\beta\alpha}^b = \delta_{ab} T_F \quad T_F = \frac{1}{2}$$

C_F, C_A describe the effective color charge of quark/gluon.

Casimir operator of $SU(N_C)$,
here: $SU(N_C=3)$.

Casimir operator of adjoint representation of gluons.

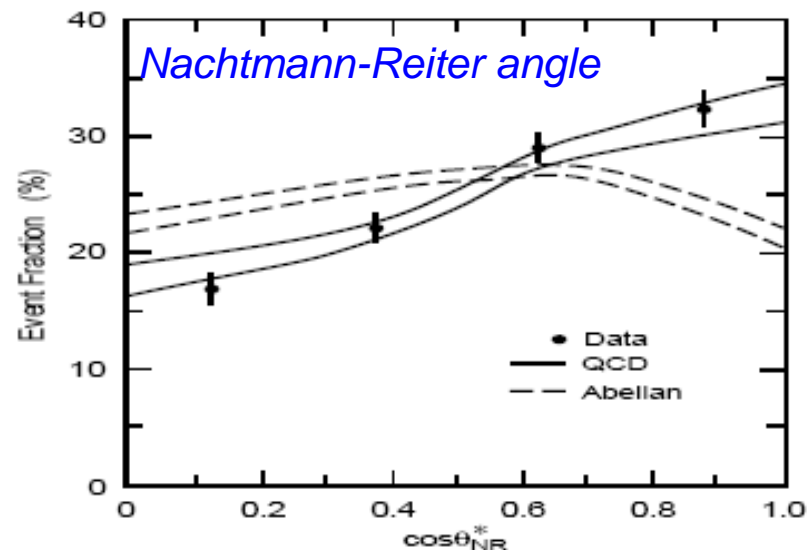
$$\frac{T_F}{C_F} = \frac{N_C}{N_A} = \frac{\# \text{ colors}}{\# \text{ gluons}}$$

Angular correlation of jets in 4-jet events

4-jet cross section:

$$\frac{1}{\sigma_0} d\sigma^4 = \left(\frac{\alpha_s C_F}{\pi}\right)^2 \left[F_A + \left(1 - \frac{1}{2} \frac{N_C}{C_F}\right) F_B + \frac{N_C}{C_F} F_C \right] \\ + \left(\frac{\alpha_s C_F}{\pi}\right)^2 \left[\frac{T_F}{C_F} N_f F_D + \left(1 - \frac{1}{2} \frac{N_C}{C_F}\right) F_E \right]$$

$F_{A,B,C,D,E}$ are kinematic functions



Exploiting the angular distribution of 4-jets:

- Bengston-Zerwas angle

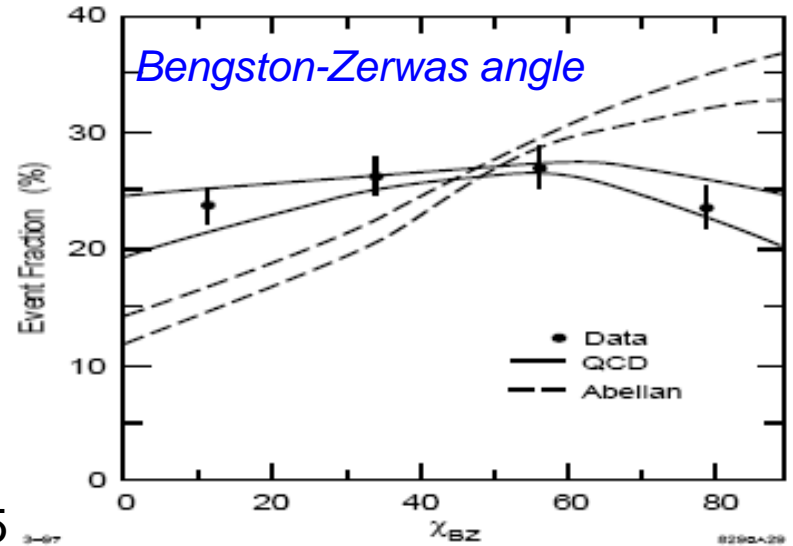
$$\cos \chi_{BZ} \propto (\vec{p}_1 \times \vec{p}_2) \cdot (\vec{p}_3 \times \vec{p}_4)$$

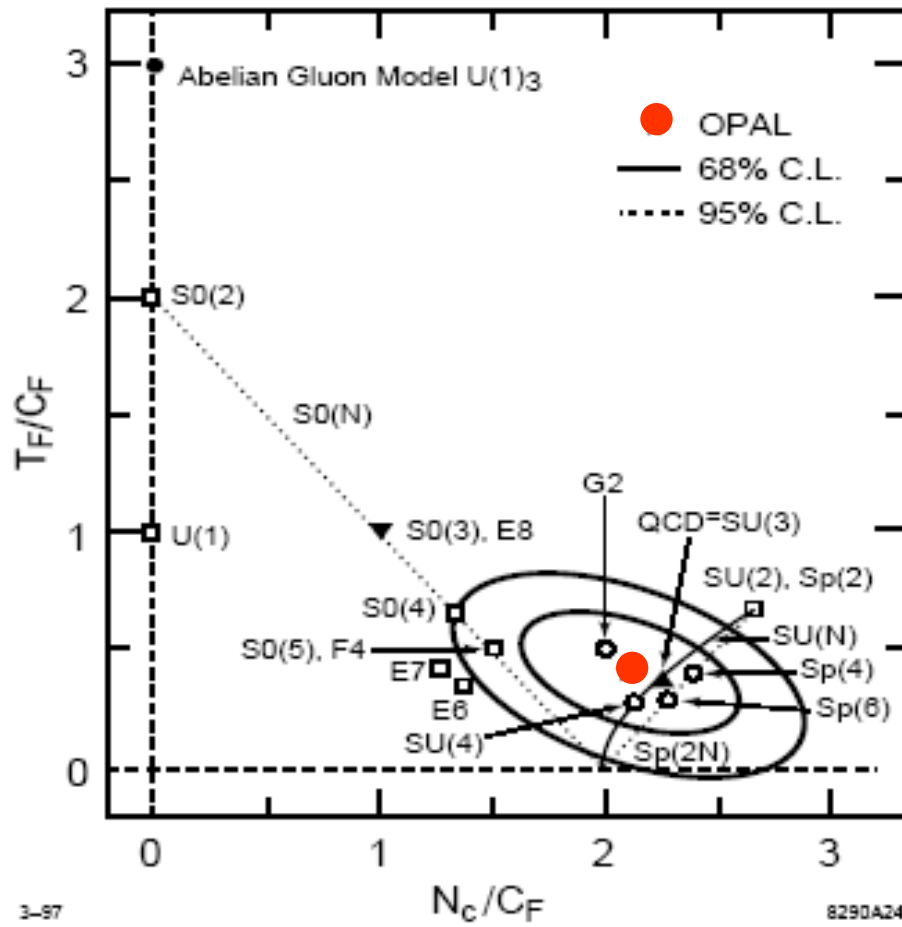
- Nachtmann-Reiter angle

$$\cos \theta_{NR} \propto (\vec{p}_1 - \vec{p}_2) \cdot (\vec{p}_3 - \vec{p}_4)$$

Allows to measure the ratios T_F/C_F and N_C/C_F

SU(3) predicts: $T_F/C_F = 0.375$ and $N_C/C_F = 2.25$



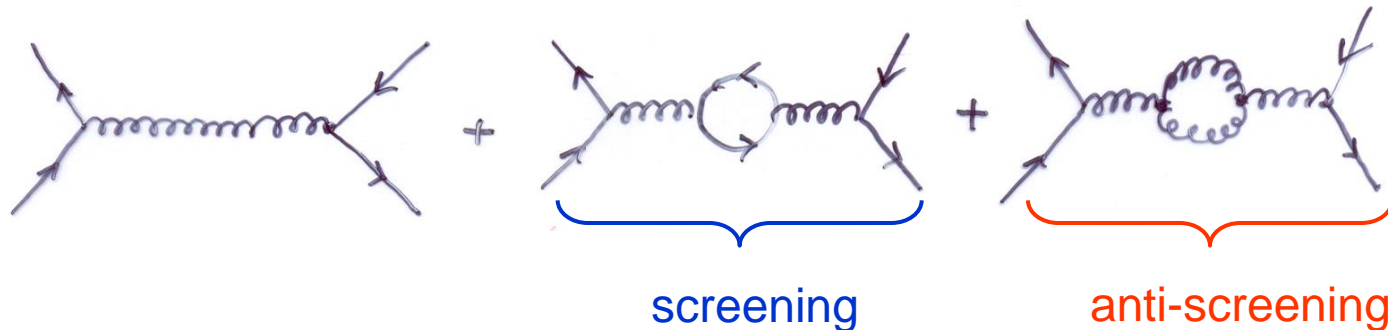


Confirms QCD prediction (SU(3)) and gluon self-coupling:

$$T_F/C_F = 0.375 \text{ and } N_c/C_F = 2.25$$

2. “Running” of the strong coupling α_s

Propagator corrections:



Strong coupling $\alpha_s(Q^2)$

$$\alpha_s(Q^2) = \frac{\alpha_s(\mu^2)}{1 + \alpha_s(\mu^2) \underbrace{\frac{1}{12\pi} (33 - 2n_f)}_{\beta_0} \log \frac{Q^2}{\mu^2}}$$

$$\beta_0 = \frac{1}{12\pi} (33 - 2n_f)$$

n_f = active quark flavors
 μ^2 = renormalization scale
conventionally $\mu^2 = M_Z^2$

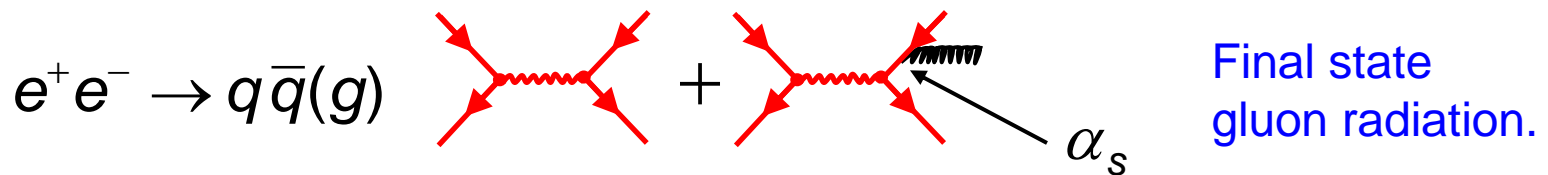
$$\alpha_s(Q^2) = \frac{1}{\beta_0 \log(Q^2/\Lambda_{QCD}^2)}$$

with $\Lambda_{QCD} \approx 200 \text{ MeV}$
scale at which perturbation theory diverges

Measurement of Q^2 dependence of α_s

→ α_s measurements are done at given scale Q^2 : $\alpha_s(Q^2)$

a) α_s from total hadronic cross section



$$\sigma_{had}(s) = \sigma_{had}^{QED}(s) \left[1 + \frac{\alpha_s(s)}{\pi} + 1.411 \cdot \frac{\alpha_s(s)^2}{\pi^2} + \dots \right]$$

$$R_{had} = \frac{\sigma(ee \rightarrow \text{hadrons})}{\sigma(ee \rightarrow \mu\mu)} = 3 \sum Q_q^2 \left\{ 1 + \frac{\alpha_s}{\pi} + 1.411 \frac{\alpha_s^2}{\pi^2} + \dots \right\}$$

→ $\alpha_s(s)$

b) α_s from hadronic event shape variables

3-jet rate: $R_3 \equiv \frac{\sigma_{3-jet}}{\sigma_{had}}$ depends on α_s

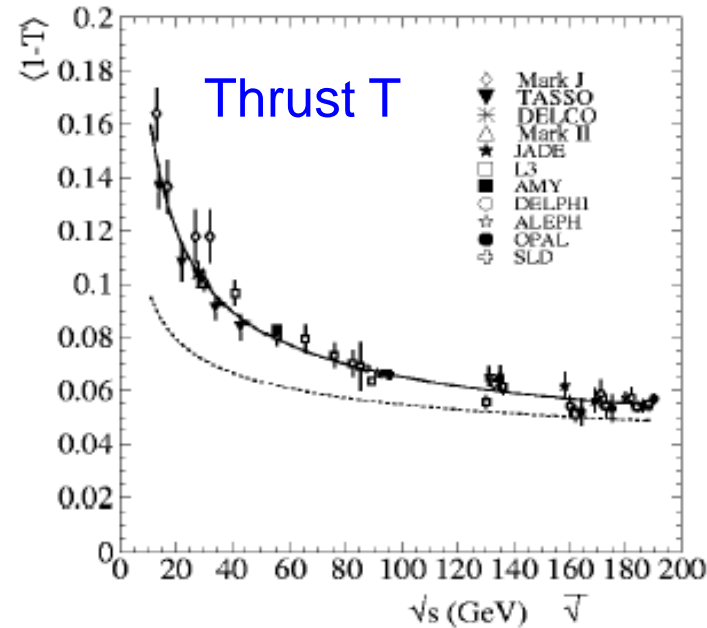
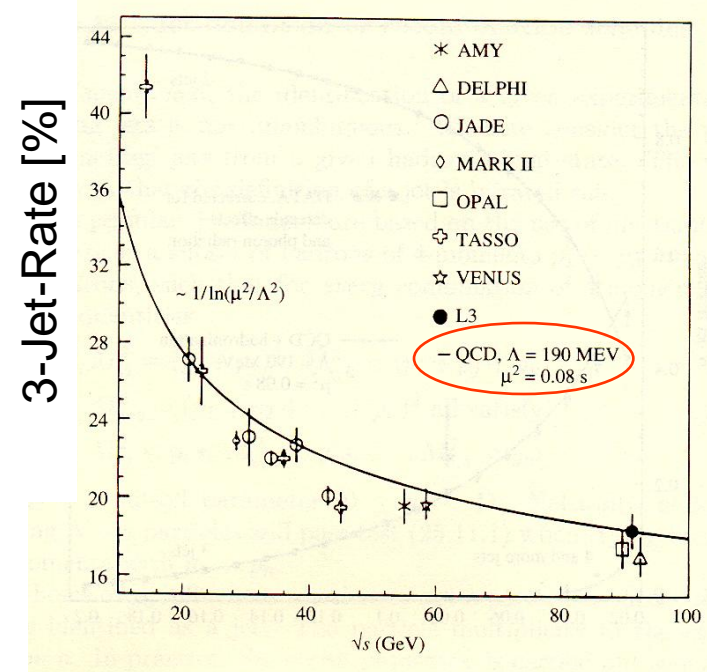
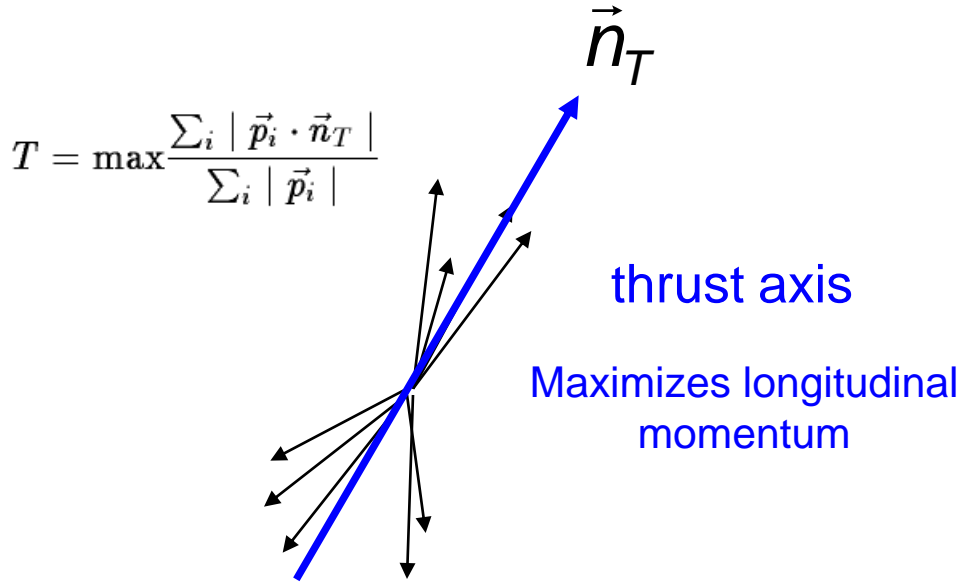
3-jet rate is measured as function of a jet resolution parameter y_{cut}

QCD calculation provides a theoretical prediction for $R_3^{\text{theo}}(\alpha_s, y_{\text{cut}})$

→ fit $R_3^{\text{theo}}(\alpha_s, y_{\text{cut}})$ to the data to determine α_s

Similarly other event shape variables (sphericity, thrust,...) can be used to obtain a prediction for α_s

$$\rightarrow \alpha_s(s)$$



c) α_s from hadronic τ decays

$$R_{had}^\tau = \frac{\Gamma(\tau \rightarrow \nu_\tau + \text{Hadrons})}{\Gamma(\tau \rightarrow \nu_\tau + e\bar{\nu}_e)} \sim f(\alpha_s)$$

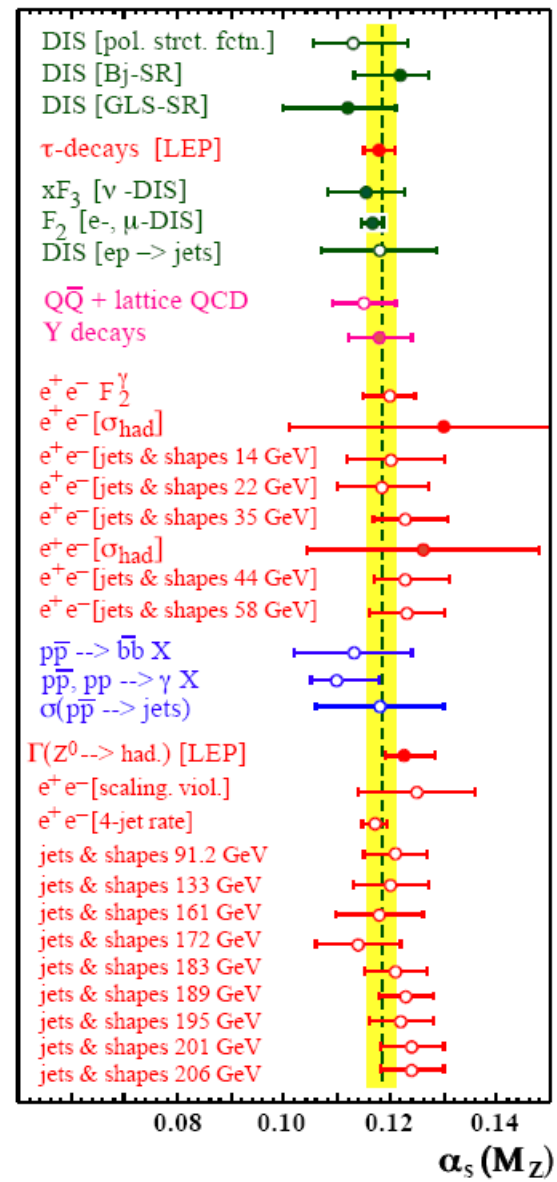
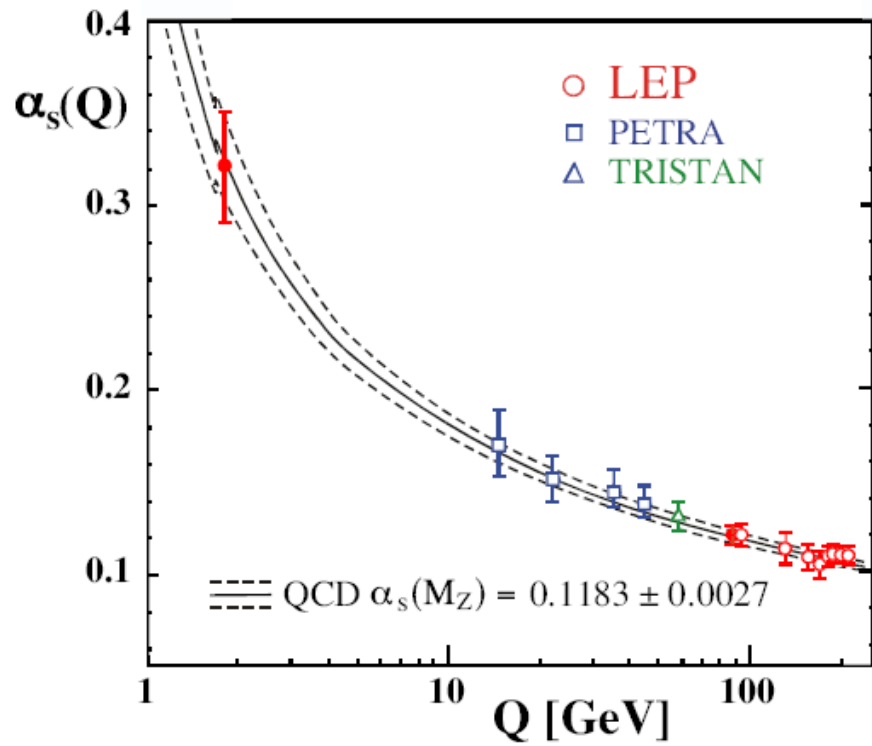
$$R_{had}^\tau = \frac{\left| \begin{array}{c} \tau^- \rightarrow \nu_\tau + W^- \\ W^- \rightarrow q\bar{q} \end{array} \right|^2 + \left| \begin{array}{c} \tau^- \rightarrow \nu_\tau + W^- \\ W^- \rightarrow q\bar{q} \text{ (with gluon loop)} \end{array} \right|^2 + \dots}{\left| \begin{array}{c} \tau^- \rightarrow \nu_\tau + W^- \\ W^- \rightarrow e^- \bar{\nu}_e \end{array} \right|^2}$$

$$R_{had}^\tau = R_{had}^{\tau,0} \left(1 + \frac{\alpha_s(m_\tau^2)}{\pi} + \dots \right)$$

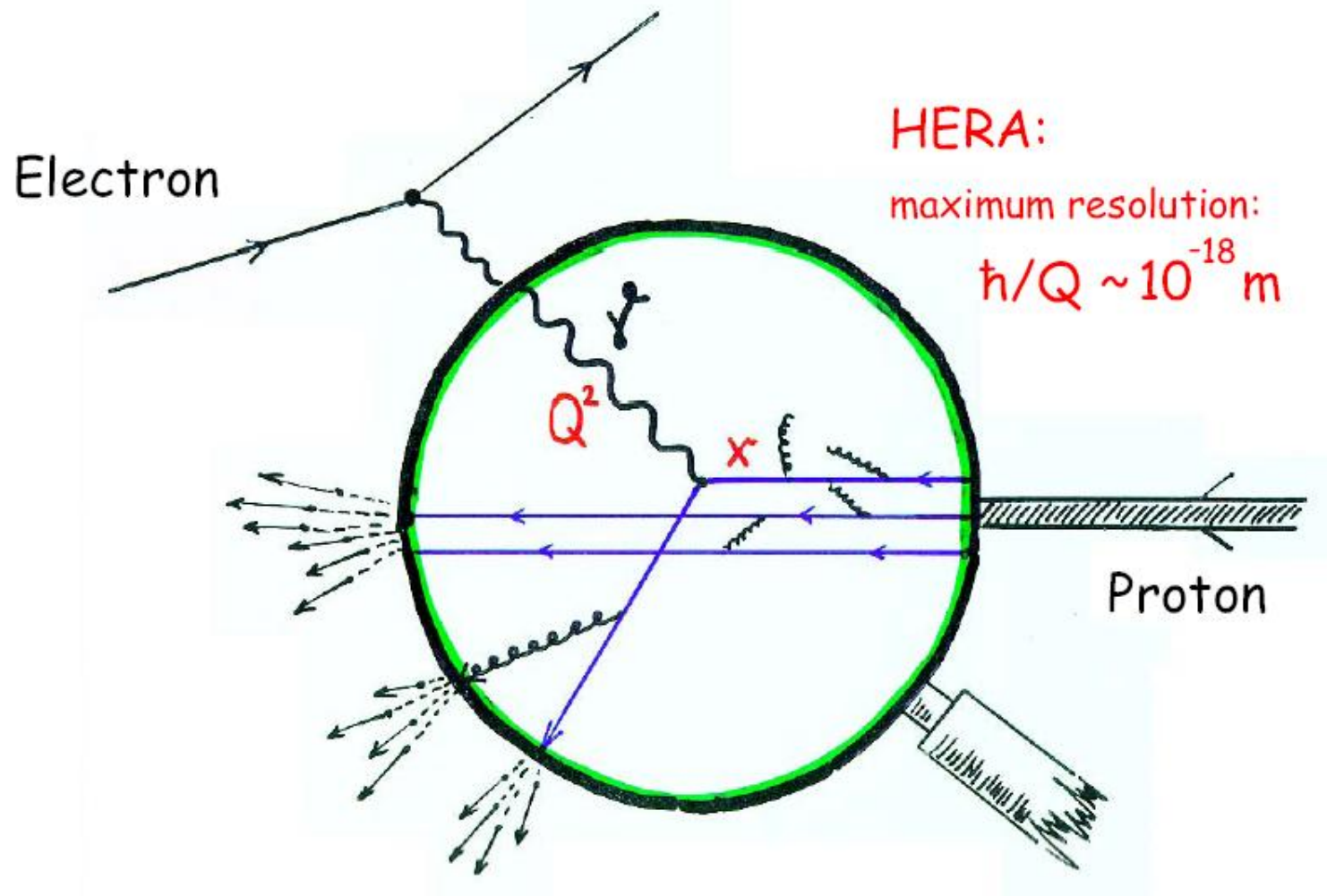
d) α_s from DIS (deep inelastic scattering)

Running of α_s and asymptotic freedom

$$\alpha_s(Q^2) = \frac{1}{\beta_0 \log(Q^2/\Lambda_{QCD}^2)}$$

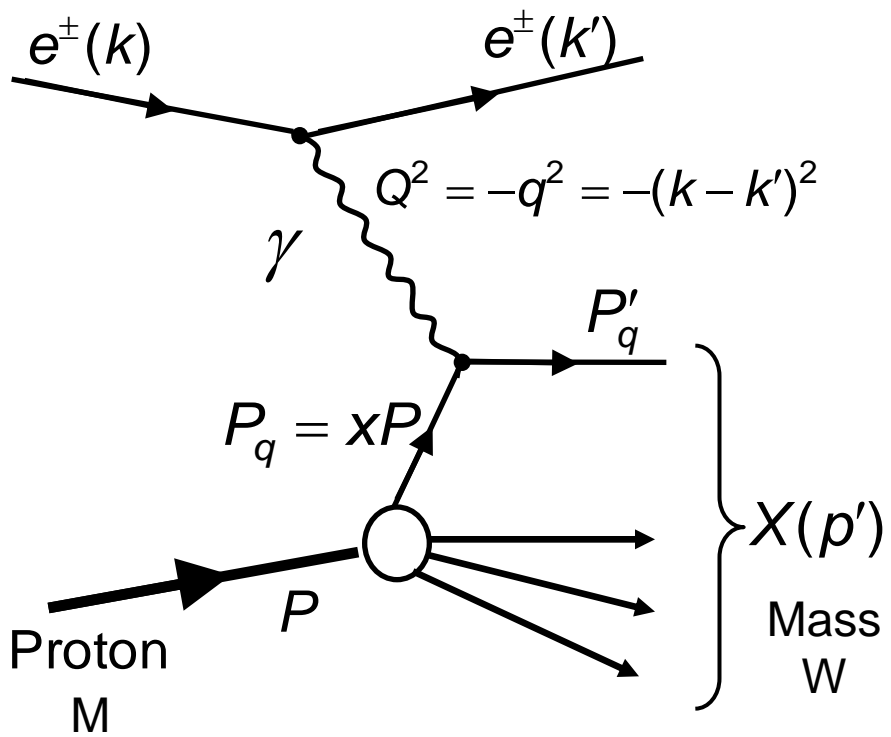


3. Study of QCD in deep inelastic scattering (DIS)



Courtesy: H.C. Schultz-Coulon

3.1 DIS in the quark parton model (QPM)



x = fractional momentum of struck quark
y = P_q/P_k = elasticity, fractional energy transfer in proton rest frame
v = $E - E'$ = energy transfer in lab

- Elastic scattering: $W = M$
 \Rightarrow only one free variable

$$\frac{Q^2}{2M\nu} = 1$$

- Inelastic scattering: $W \neq M$
 \Rightarrow scattering described by 2 independent variables

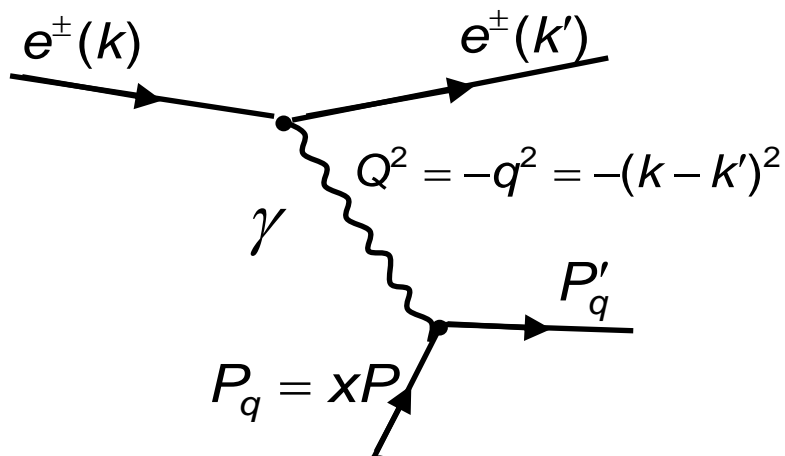
$$(E, \nu), (Q^2, x), (x, y), \dots$$

$$Q^2 = sxy \quad s = \text{CMS energy}$$

$$x = \frac{Q^2}{2M\nu} \quad (\text{Bjorken } x)$$

Cross section in quark parton model (QPM)

Elastic scattering on single quark



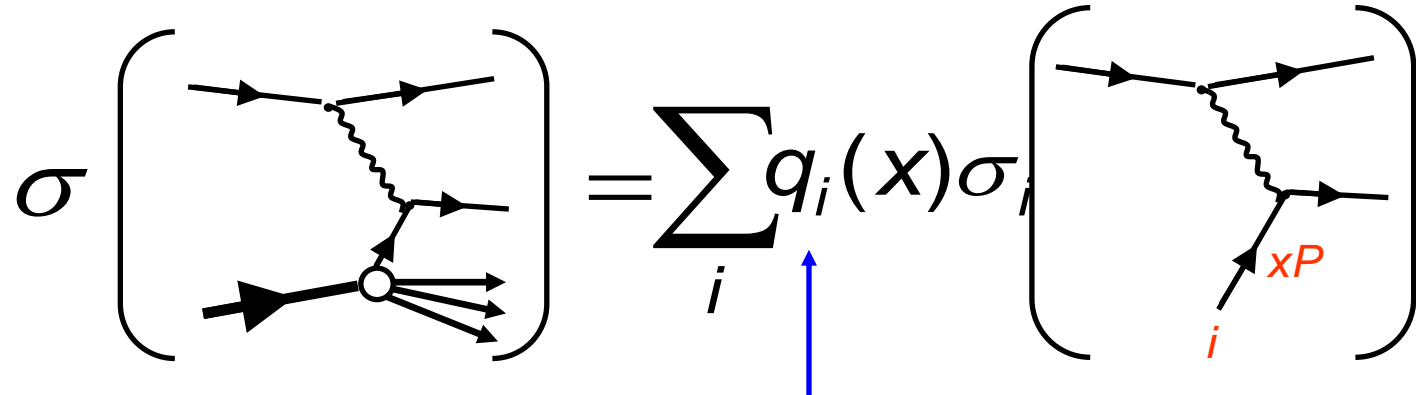
Starting point:
electron muon scattering

$$\{ \dots \}_{e\mu \rightarrow e\mu}^{elastic} = \left(\cos^2 \frac{\theta}{2} + \frac{Q^2}{2M^2} \sin^2 \frac{\theta}{2} \right)$$

Electron-quark scattering (quark momentum fraction x):

$$\frac{d\sigma}{dQ^2} = \left(\frac{4\pi\alpha^2}{Q^4} \right) \frac{E'}{E} \cdot e_i^2 \left(\cos^2 \frac{\theta}{2} + \frac{Q^2}{2x^2 M^2} \sin^2 \frac{\theta}{2} \right)$$

↑
charge



Parton density $q_i(x)dx$: Probability to find parton i in momentum interval $[x, x+dx]$

$$\frac{d^2\sigma}{dQ^2 dx} = \left(\frac{4\pi\alpha^2}{Q^4} \right) \frac{E'}{E} \cdot \sum_i \int_0^1 e_i^2 \cdot q_i(\xi) \cdot \delta(x - \xi) d\xi \left(\cos^2 \frac{\theta}{2} + \frac{Q^2}{2x^2 M^2} \sin^2 \frac{\theta}{2} \right)$$

Structure functions

$$F_2(x) = x \sum_i \int_0^1 e_i^2 q_i(\xi) \cdot \delta(x - \xi) d\xi = x \sum_i e_i^2 q_i(x)$$

$$F_1(x) = \frac{1}{2} \sum_i e_i^2 q_i(x)$$

ignore (include) anti-quarks!

$$\frac{d^2\sigma}{dQ^2dx} = \left(\frac{4\pi\alpha^2}{Q^4} \right) \frac{E'}{E} \cdot \left(\frac{F_2(x)}{x} \cos^2 \frac{\theta}{2} + 2F_1(x) \frac{Q^2}{2x^2M^2} \sin^2 \frac{\theta}{2} \right)$$

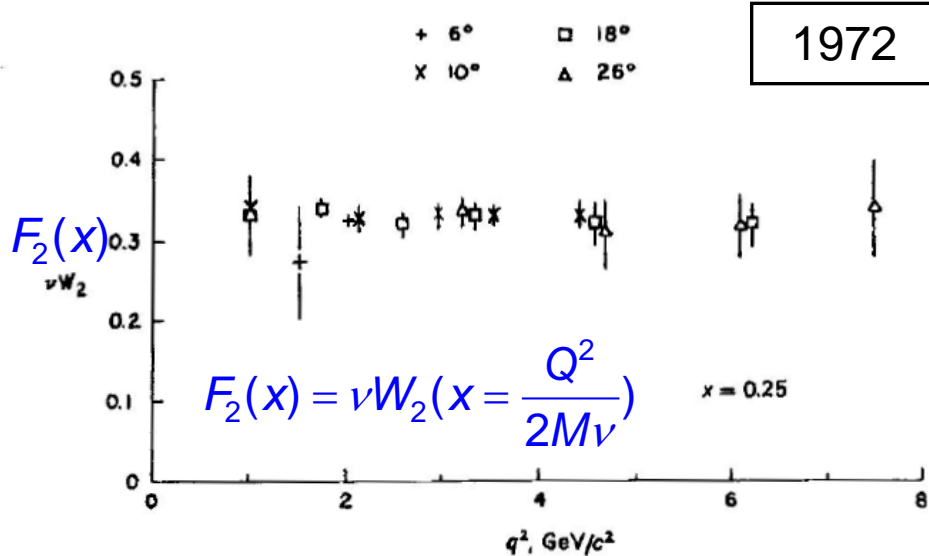


Kinematical relations

$$\frac{d^2\sigma}{dQ^2dx} = \left(\frac{4\pi\alpha^2}{Q^4x} \right) \cdot ((1-y)F_2(x) + xy^2F_1(x))$$

Deep inelastic electron-proton scattering:

- Free partons: $F_2=F_2(x) \Leftrightarrow$ “scaling”
- Spin $\frac{1}{2}$ partons: $2xF_1(x) = F_2(x)$
(Callan-Gross relation)



Scaling

Structure function F_2 ($=\nu W_2$) depends only on the dimensionless variable x :

$$x = \frac{Q^2}{2M\nu}$$

→ **Scale invariance: “scaling”**

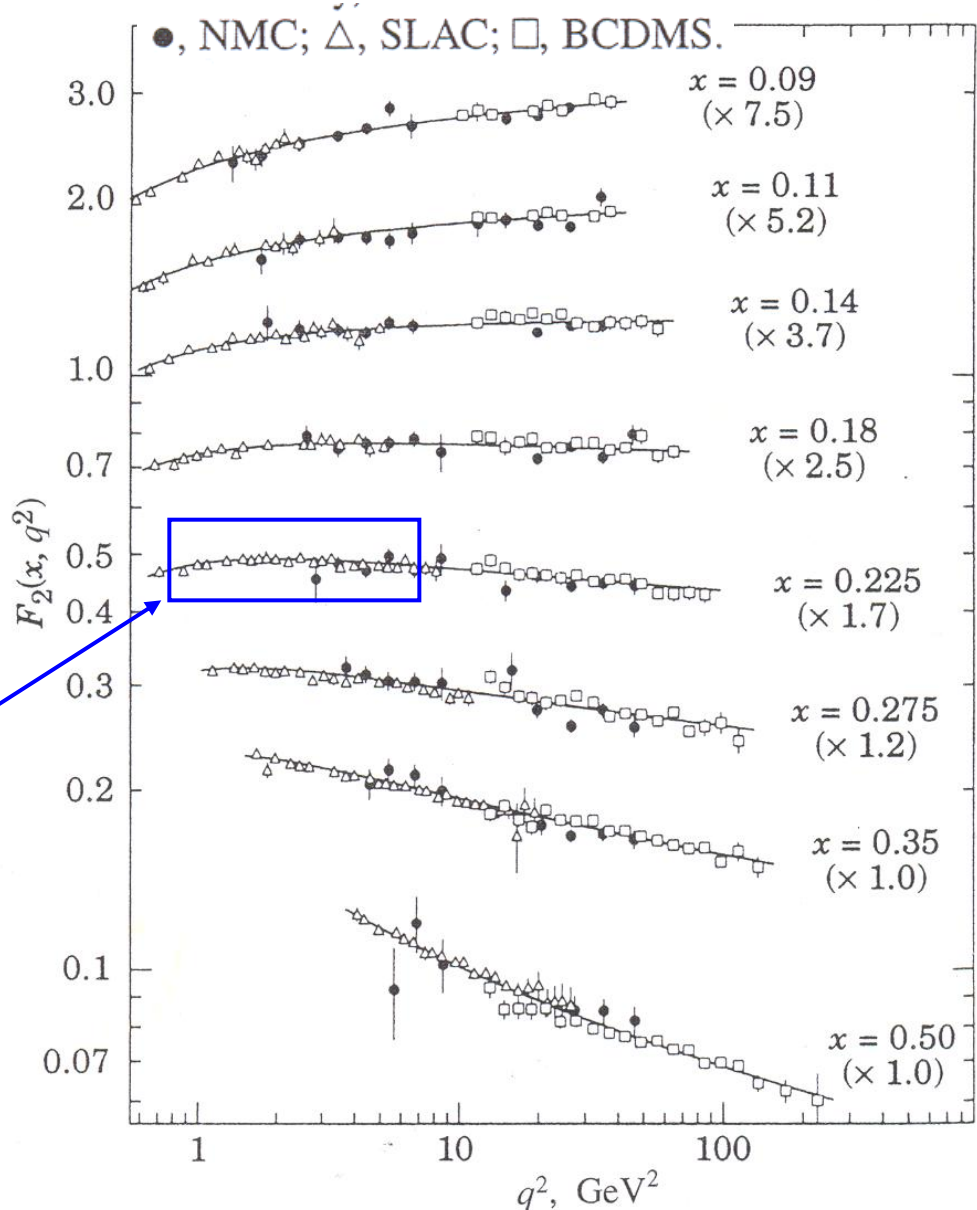
Indicates elastic scattering at point-like free constituents of the proton: partons

3.2 Scaling violation

Structure function:

$$F_2 = F_2(x, Q^2) = x \sum_i e_i^2 q_i(x)$$

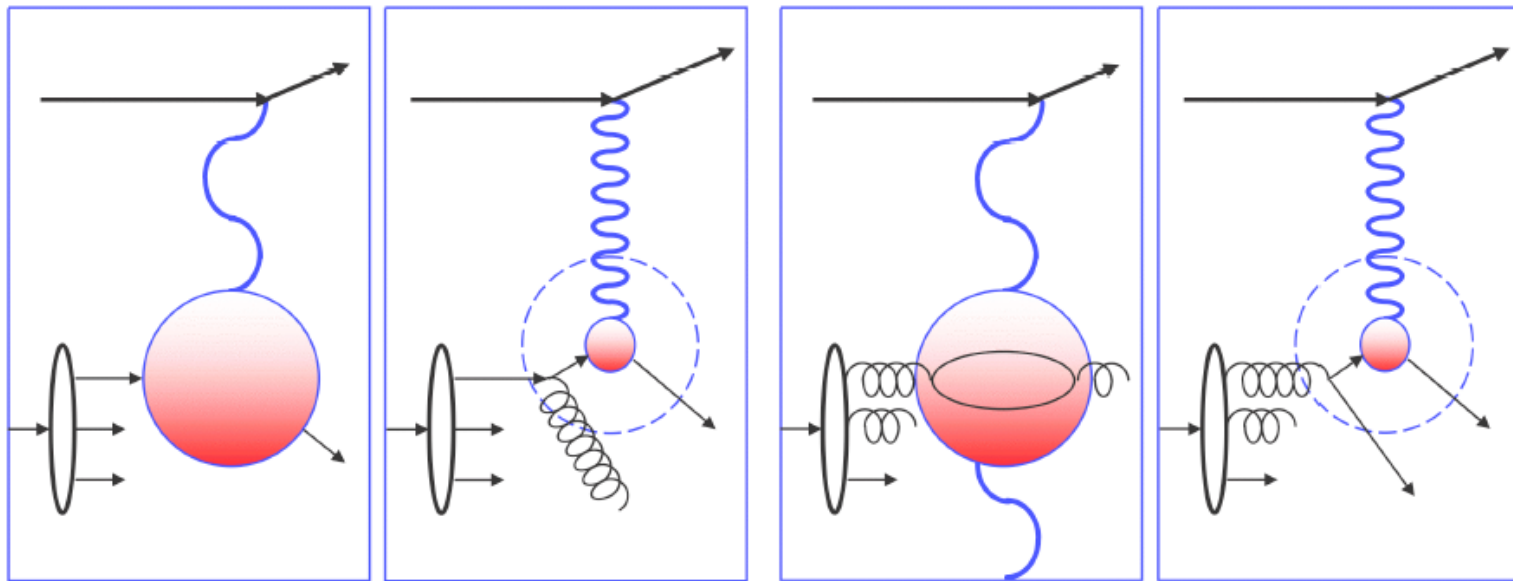
Region of 1st SLAC measurement (1972)



QCD explains observed scaling violation

Large x: valence quark scattering

Small x: Gluon+sea quark scattering



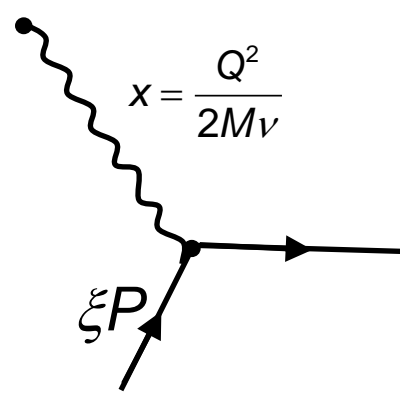
$Q^2 \uparrow \Rightarrow F_2 \downarrow$ for fixed x

$Q^2 \uparrow \Rightarrow F_2 \uparrow$ for fixed (small) x

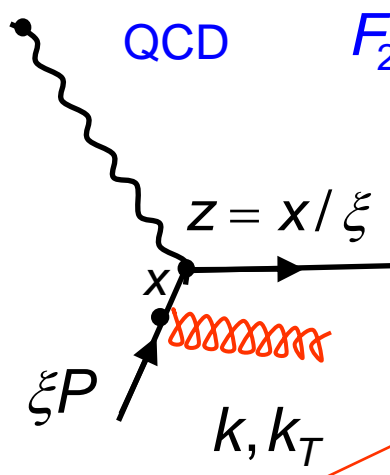
Scaling violation is one of the clearest manifestation of radiative effect predicted by QCD.

Quantitative description of scaling violation

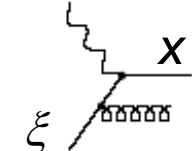
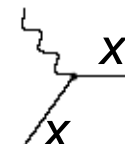
Quark Parton Model



$$F_2(x) = x \sum_i e_i^2 \int_0^1 q_i(\xi) \cdot \delta(x - \xi) d\xi = x \sum_i e_i^2 q_i(x)$$



$$F_2(x, Q^2) = x \sum_i e_i^2 \int_0^1 \frac{d\xi}{\xi} q_i(\xi) \cdot \left[\delta(1 - \frac{x}{\xi}) + \frac{\alpha_s}{2\pi} P_{qq}(\frac{x}{\xi}) \log \frac{Q^2}{\mu_0^2} \right]$$



$$\begin{aligned} & \sim \frac{\alpha_s}{2\pi} P_{qq}(z) \int_{\mu_0^2}^{Q^2} \frac{dk_T^2}{k_T^2} \\ & \sim \frac{\alpha_s}{2\pi} P_{qq}(z) \log \left(\frac{Q^2}{\mu_0^2} \right) \end{aligned}$$

In the limit of small
irradiation angle

P_{qq} probability of a quark
to emit gluon and
becoming a quark with
momentum reduced by
fraction z .

μ^0 cutoff parameter

$$\delta(ax) = \frac{1}{|a|} \delta(x)$$

Changing to the quark (parton) densities:

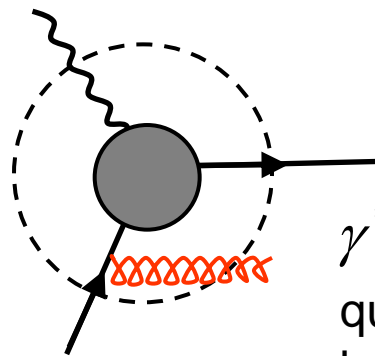
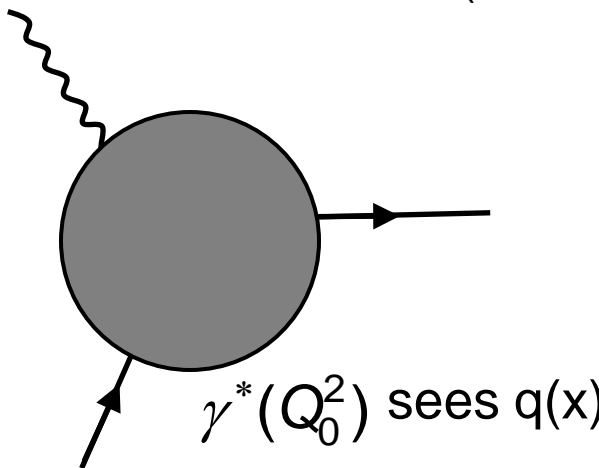
$$q_i(x, Q^2) = q_i(x) + \underbrace{\frac{\alpha_s}{2\pi} \log \frac{Q^2}{\mu_0^2} \int_0^1 \frac{d\xi}{\xi} q_i(\xi) P_{qq}\left(\frac{x}{\xi}\right)}_{\Delta q(x, Q^2)}$$

Integro-differential equation for $q(x, Q^2)$:

$$\frac{d}{d \log Q^2} q(x, Q^2) = \frac{\alpha_s}{2\pi} \int_0^1 \frac{d\xi}{\xi} q(\xi, Q^2) P_{qq}\left(\frac{x}{\xi}\right)$$

We have
ignored gluon
splitting

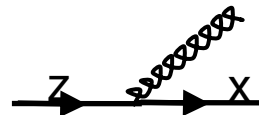
DGLAP evolution equation
(Dokshitzer, Gribov, Lipatov, Altarelli, Parisi, 1972 – 1977)



$\gamma^*(Q^2 > Q_0^2)$ sees that
quarks $q(x)$ are surrounded
by softer quarks

Evolution of parton densities (quarks and gluons)

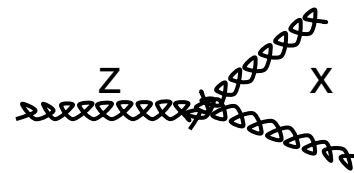
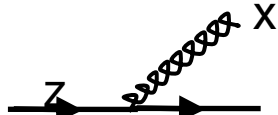
evolution of quark density with $\ln Q^2$



$$\frac{\partial q(x, Q^2)}{\partial \ln Q^2} = \frac{\alpha_s}{2\pi} \int_x^1 \frac{dz}{z} \left[q(z, Q^2) P_{qq} \left(\frac{x}{z} \right) + g(z, Q^2) P_{qg} \left(\frac{x}{z} \right) \right]$$

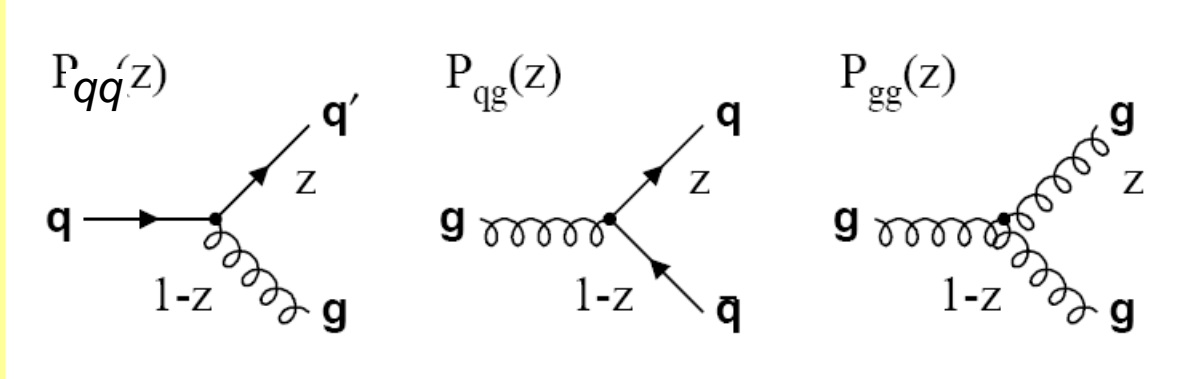
$$\frac{\partial g(x, Q^2)}{\partial \ln Q^2} = \frac{\alpha_s}{2\pi} \int_x^1 \frac{dz}{z} \left[q(z, Q^2) P_{gq} \left(\frac{x}{z} \right) + g(z, Q^2) P_{gg} \left(\frac{x}{z} \right) \right]$$

evolution of gluon density with $\ln Q^2$



Splitting functions: Probability that a parton (quark or gluon) emits a parton (**q, g**) with momentum fraction $\varepsilon=x/z$ of the parent parton.

Splitting functions are calculated as power series in α_s up to a given order:



$$P_{ij}(z, \alpha_s) = P_{ij}^0(z) + \frac{\alpha_s}{2\pi} P_{ij}^1(z) + \dots$$

In leading order: $P_{ij}(z, \alpha_s) \equiv P_{ij}^0(z)$

$$P_{qq}(z) = \frac{4}{3} \frac{1+z^2}{1-z}$$

$$P_{qg}(z) = \frac{4}{3} \frac{1+(1-z)^2}{z}$$

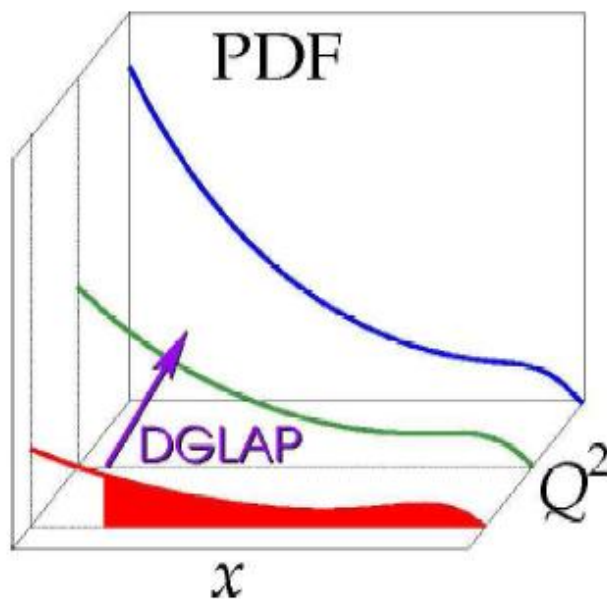
$$P_{qg}(z) = \frac{z^2 + (1-z)^2}{2}$$

$$P_{gg}(z) = 6 \left(\frac{z}{1-z} + \frac{1-z}{z} + z(1-z) \right)$$

DGLAP Evolution (“symbolic”):

$$\frac{\partial}{\partial \log Q^2} \begin{bmatrix} q(x, Q^2) \\ g(x, Q^2) \end{bmatrix} = \frac{\alpha_s}{2\pi} \begin{bmatrix} P_{q/q} & P_{q/g} \\ P_{g/q} & P_{g/g} \end{bmatrix} \otimes \begin{bmatrix} q(x, Q^2) \\ g(x, Q^2) \end{bmatrix}$$

The diagram shows the DGLAP evolution equation. On the left, the derivative of the PDFs with respect to the logarithm of the scale is given. The right side consists of a convolution (indicated by \otimes) between the initial PDFs and a matrix of evolution kernels. The kernels are represented by Feynman diagrams: $P_{q/q}$ (quark-to-quark), $P_{q/g}$ (quark-to-gluon), $P_{g/q}$ (gluon-to-quark), and $P_{g/g}$ (gluon-to-gluon). The quark and gluon fields are labeled x and z respectively.



$$P \otimes f(x, Q^2) = \int_x^1 \frac{dz}{z} P\left(\frac{x}{z}\right) f(z, Q^2)$$

QCD evolution:

QCD predicts the PDF behavior for a scale Q^2 once the PDF was measured at another scale.

HERA

e^\pm $\xrightarrow{30\text{ GeV}}$ p $\xleftarrow{900\text{ GeV}}$

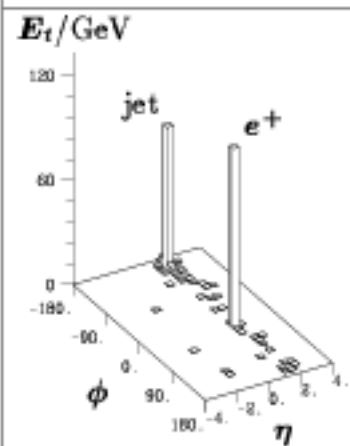
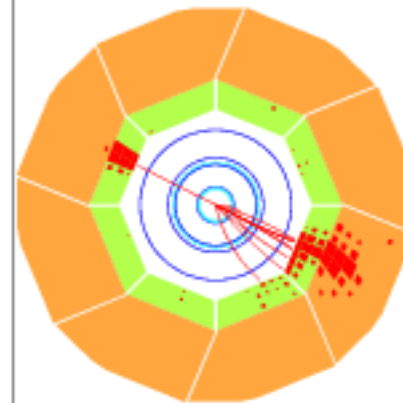
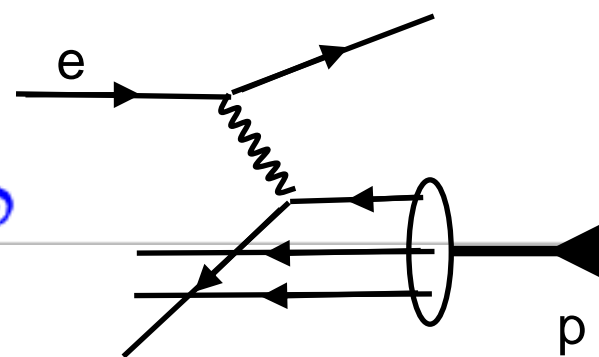
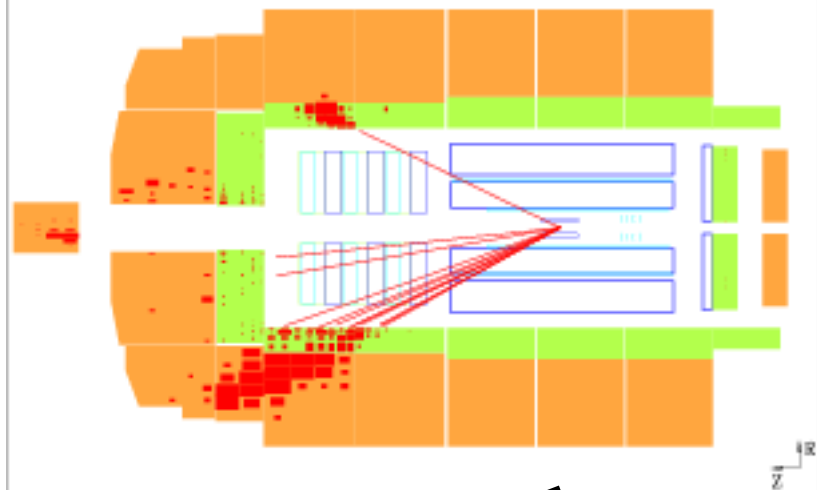
$$s = 4E_e E_p \approx 10^5 \text{ GeV}^2$$



H1 Run 122145 Event 69506

Date 19/09/1995

$$Q^2 = 25030 \text{ GeV}^2, \quad y = 0.56, \quad M = 211 \text{ GeV}$$



Measurement of the parton densities / F_2

$$\frac{d^2\sigma}{dx dQ^2} = \left(\frac{2\pi\alpha^2}{x Q^4} \right) \cdot \left(2 \cdot (1-y) F_2(x, Q^2) + y^2 F_2(x, Q^2) \right)$$



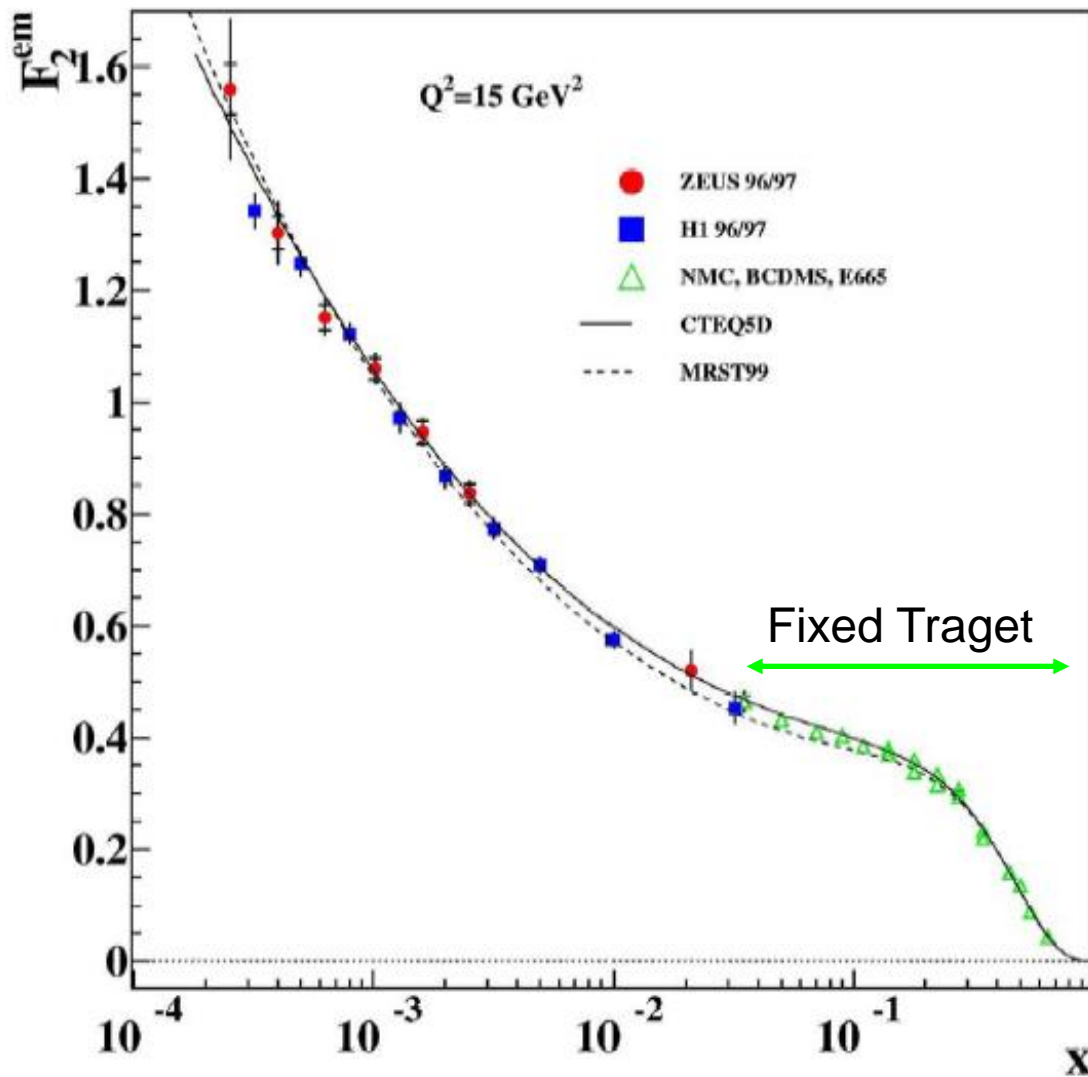
e.g. for $y=1$

$$Q^2 = sxy$$

$$\frac{d^2\sigma}{dx dQ^2} = \left(\frac{2\pi\alpha^2}{x Q^4} \right) \cdot F_2(x, Q^2)$$

$$F_2(x, Q^2) = x \sum_q e_q^2 [q(x, Q^2) + \bar{q}(x, Q^2)]$$

ZEUS+H1



$$F_2(x)$$

Large increase of $F_2(x)$ for very small x - unexpected

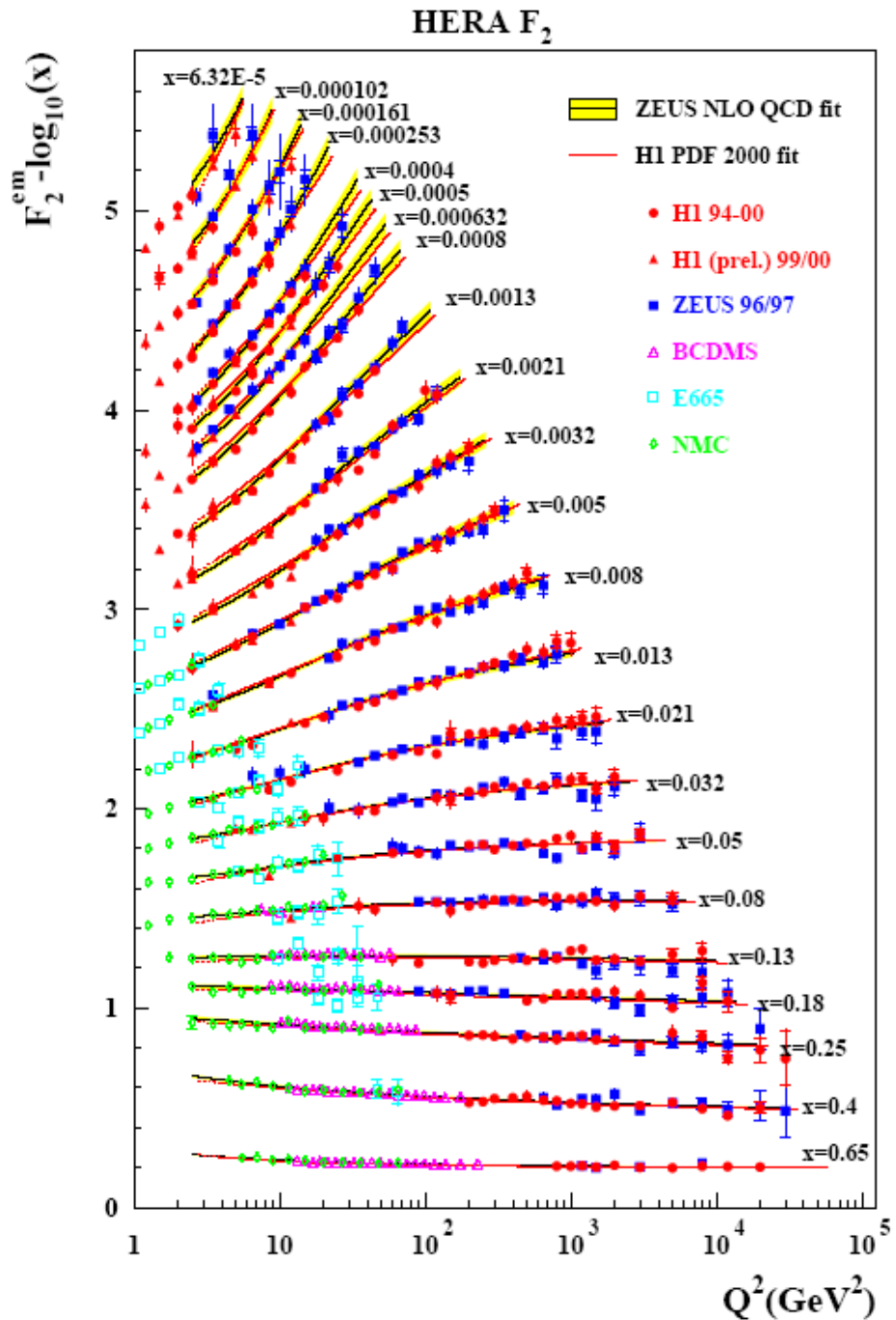


When does the rise stop ??

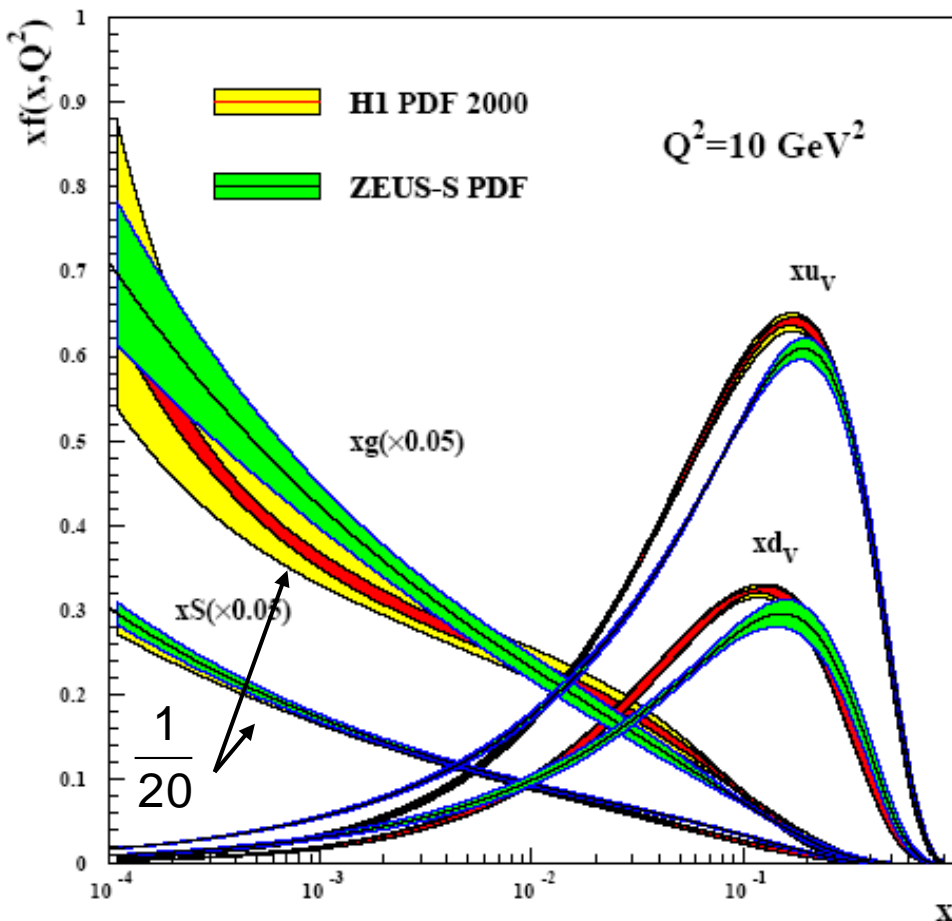
$$F_2(x, Q^2)$$



Q^2 dependence is correctly described by QCD evolution



Structure of the proton as seen by HERA



$$\# \text{ Valenzquarks} = \int u_v(x) + d_v(x) dx = 3$$

$$\# \text{ Gluonen} = \int g(x) dx > 30$$

